Mechanism for neuronal spike generation by small and large ion channel clusters

Shangyou Zeng and Peter Jung
Department of Physics and Astronomy, Ohio University, Athens, Ohio 45701, USA
(Received 20 November 2003; published 7 July 2004)

Neuronal action potentials are generated by clusters of ion channels between the Hillock and the first segment. If the clusters comprise a large number of sodium and potassium channels, action potentials are generated if the membrane potential exceeds a threshold of about −55 mV. Such behavior is well described by an excitable model such as, for example, the Hodgkin-Huxley equations. In this paper we show through stochastic modeling that if the size of the generating ion channel cluster is small, action potentials are generated regardless of whether the membrane potential is below or above the excitation threshold. Action potential generation is then determined by single-channel kinetics. We further show that this switch in generation mechanism manifests itself in peculiar statistical properties of the generated spike trains at small cluster sizes.

DOI: 10.1103/PhysRevE.70.011903 PACS number(s): 87.16.Uv, 87.15.Ya

I. INTRODUCTION

Conductance-based models for the transmembrane voltage of neurons—pioneered in the seminal paper by Hodgkin and Huxley [1]—are the cornerstone of modern computational neuroscience. The essential idea is that the conductance of the membrane is determined by the conductance of the potassium and sodium systems which in turn is determined by the membrane potential. The nonlinear dependence of the sodium and potassium conductance on the membrane potentials generates action potentials that travel down the axon to contact other neurons. The conductance of sodium and potassium through the membrane is facilitated by specific ion channels that individually switch stochastically between the open and the closed state as demonstrated by Neher and Sakman [2]. Experiments show that individual ion channels open and close randomly with membrane-voltage dependent opening and closing rates [2,3]. The deterministic Hodgkin-Huxley equations [1] describe the dynamics of the membrane potential if the number of ion channels is very large, i.e., when conductance fluctuations are negligible. If the action potentials are generated by a cluster of sodium and potassium channels that comprises few channels only, stochastic effects become important, giving rise to spontaneous spiking [4,5]. In such situations, stochastic Hodgkin-Huxley equations have to be employed to describe the transmembrane potential [6–11]. When the ion channel number is large, the stochastic Hodgkin-Huxley equations will approach the conventional Hodgkin-Huxley equations [10,11]. The effects of channel noise (as a function of the size of the ion channel cluster) have been studied recently in the context of the coherence of the generated neuronal spike train [12,13]. Besides channel noise, other sources of noise are important. Synaptic noise is generated by stochastic effects in the transport of neurotransmitter through the synaptic cleft as well as by the relative small number of postsynaptic receptors. Furthermore, a neuron is often contacted by a large number of other neurons whose signals can act like a noise source [14]. Other sources of noise are ligand-gated ion channels [15]. In this paper we report on the differences of the mechanism of action potential generation by small and large ion channel clusters and how these differences are expressed in the statistical properties of the neuronal spike train. We further explore the role of synaptic noise on the generation of action potentials by a small and large clusters of ion channels in the neuronal membrane. Since synaptic noise is extrinsic to the ion channel processes that generate the action potentials, it appears as noise term in the equation for the membrane voltage. Intrinsic channel noise appears in the equations for the gating variables [10,11]. In Sec. II, we describe the stochastic Hodgkin-Huxley model in the presence of channel noise and synaptic noise. In Sec. III, four algorithms are described that are commonly used to evaluate the stochastic Hodgkin-Huxley model, the straightforward simulation of each individual gate of each channel, a Markov process mimicking transitions between occupation-number states of the ion channel cluster, the Gillespie method, and a Langevin approach. In Sec. IV we describe results for the spiking rates, variability of the spiking and temporal coherence of the generated spike trains. In Sec. V our results are summarized.

II. MODEL

We adopt the classic model for the ion channels introduced by Hodgkin and Huxley that models the potassium channel by four identical gates that stochastically switch between an open state and a closed state. The open probabilities p_n for the four gates $n=1,2,3,4$ are described by the rate equations

$$\dot{p}_n(t) = -[\alpha_K(v) + \beta_K(v)]p_n(t) + \alpha_K(v), \tag{1}$$

where $\alpha_K(v)$ and $\beta_K(v)$ are the membrane-voltage v dependent opening and closing rates

$$\alpha_K(v) = \frac{0.01(10-v)}{\exp[(10-v)/10]-1}, \quad \beta_K(v) = 0.125\ \exp\left(-\frac{v}{80}\right). \tag{2}$$

The transmembrane voltage v is measured here and in all equations below in millivolt with respect to the physiologic cellular resting potential of −65 mV. The potassium channel is open only when all four gates are open, i.e., with probability $p_1p_2p_3p_4$.

 ©2004 The American Physical Society

The sodium channel consists of four gates. Three identical fast gates increase their opening probability q_1, q_2, q_3 when the voltage v becomes larger than the resting potential. The slower fourth deactivation gate decreases its open probability q_4 when the membrane potential increases. The gate variables obey the following rate equations:

$$\dot{q}_n(t) = -[\alpha^f_{\mathrm{Na}}(v) + \beta^f_{\mathrm{Na}}(v)]q_n(t) + \alpha^f_{\mathrm{Na}}(v)$$

$$\dot{q}_4(t) = -[\alpha^s_{\mathrm{Na}}(v) + \beta^s_{\mathrm{Na}}(v)]q_4(t) + \alpha^s_{\mathrm{Na}}(v), \tag{3}$$

with the opening and closing rates

$$\alpha^f_{\mathrm{Na}}(v) = \frac{0.1(25-v)}{\exp[(25-v)/10]-1}, \quad \beta^f_{\mathrm{Na}}(v) = 4.0\ \exp\left(-\frac{v}{18}\right),$$

$$\alpha^s_{\mathrm{Na}}(v) = 0.07\ \exp\left(-\frac{v}{20}\right), \quad \beta^s_{\mathrm{Na}}(v) = \frac{1}{\exp[(30-v)/10]+1}. \tag{4}$$

The membrane voltage is measured in millivolt with respect to the resting potential.

Although each individual ion channel opens and closes independently, the opening and closing rates (for the n gate, they are α_n and β_n) are regulated by the same membrane potential. As a consequence all ion channels are globally coupled through the membrane potential. For the density of the sodium and potassium channels (number of channels per area) we use $\rho_{\mathrm{Na}} = 60/\mu\mathrm{m}^2$ and $\rho_{\mathrm{K}} = 20/\mu\mathrm{m}^2$, respectively. The single-channel conductances of the sodium and potassium channels are given by $\gamma_{\mathrm{Na}} = \gamma_{\mathrm{K}} = 20$ pS. Except for $\rho_{\mathrm{K}} = 20/\mu\mathrm{m}^2$ these values have been reported for the giant squid axon [1]. Using a membrane capacitance of $1\ \mu\mathrm{F/cm}^2$ we end up with the following equation for the membrane potential:

$$\dot{v} = -\left(\frac{N^{open}_{\mathrm{K}}}{\tau_{\mathrm{K}}N_{\mathrm{K}}}(v - v^{rev}_{\mathrm{K}}) + \frac{N^{open}_{\mathrm{Na}}}{\tau_{\mathrm{Na}}N_{\mathrm{Na}}}(v - v^{rev}_{\mathrm{Na}}) + \frac{1}{\tau_L}(v - v_l)\right), \tag{5}$$

where $v^{rev}_{\mathrm{K}} = -12$ mV, $v^{rev}_{\mathrm{Na}} = 115$ mV, and $v_l = 10.6$ mV denote reversal potentials of the potassium systems, sodium system, and leakage system, respectively. The time constants are given by

$$\tau_{\mathrm{K}} = \frac{1}{36}\mathrm{ms}$$

$$\tau_{\mathrm{Na}} = \frac{1}{120}\mathrm{ms}$$

$$\tau_L = 3.3 \quad \mathrm{ms}. \tag{6}$$

The numbers of open K^+ and Na^+ channels, N^{open}_{K} and N^{open}_{Na}, respectively, have to be determined as a function of time by stochastic simulations with methods described in the following section.

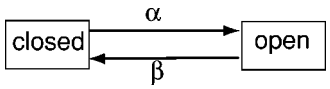

FIG. 1. Kinetic scheme of a two-state channel.

The time scale of synaptic noise is about one order of magnitude smaller than channel noise (see, e.g., in Ref. [16]). Thus we can consider synaptic noise as Gaussian white noise $\xi_s(t)$ with

$$\langle \xi_s(t) \rangle = 0,$$

$$\langle \xi_s(t)\xi_s(t') \rangle = \sigma^2 \delta(t-t'), \tag{7}$$

where σ describes the strength of the synaptic noise. Since synaptic leads to events that are integrated, it has to be added to the right-hand side of Eq. (5), i.e.,

$$\dot{v} = -\left(\frac{N^{open}_{\mathrm{K}}}{\tau_{\mathrm{K}}N_{\mathrm{K}}}(v - v^{rev}_{\mathrm{K}}) + \frac{N^{open}_{\mathrm{Na}}}{\tau_{\mathrm{Na}}N_{\mathrm{Na}}}(v - v^{rev}_{\mathrm{Na}}) + \frac{1}{\tau_L}(v - v_l)\right) + \xi_s(t). \tag{8}$$

III. METHODS

To integrate Eq. (8), the numbers of open sodium and potassium channels have to be determined at each instant. It is assumed that the subunits of the sodium and potassium channels are not cooperative and that they switch between the open and closed states according to a Markov process. There are several methods to simulate the patch of ion channels. Each method has some advantages and disadvantages.

A. Simple stochastic method

This method assumes that all gates open and close according to a two-state Markov process with voltage dependent opening and closing rates. For example, the two-state Markov process of a single gate is sketched in Fig. 1, where the transition rate α and β are the opening and closing rates of the subunit. If the gate is closed at time t, it will open with the probability $\alpha\delta t$ and remain closed with probability $1-\alpha\delta t$ in the time interval $t, t+\delta t$ for sufficiently small δt, i.e., $\delta_t \ll 1/\alpha$. If the gate is open at time t, it will close with the probability $\beta\delta t$ and remain open with probability $1-\beta\delta t$ in the time interval $t, t+\delta t$ for sufficiently small δt, i.e., $\delta_t \ll 1/\beta$. We update the state of each gate by drawing a random number r from the unit interval from a uniform distribution. If the gate is closed at time t and $r < \alpha\delta t$, the gate remains closed while it opens if $r > \alpha\delta t$. Similarly, if the gate is open at time t and $r < \beta\delta t$, the gate remains open while it closes if $r > \beta\delta t$. This method is obviously inefficient since many transitions of gates between the open and closed state do not change the state of the channel and thus the conductance of the channel. It is, however, the most accurate methods since no other assumptions than the Markov process have been made.

B. Markov-process for the occupation numbers

Instead of keeping track of the state of each gate, one can keep track only of the total populations of channels in each

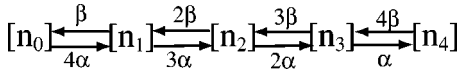

FIG. 2. Kinetic scheme for a stochastic potassium channel.

possible state [8]. Each channel has either 0, 1, 2, 3, or 4 gates open and can thus be in the corresponding states S_1, S_2, S_3, S_4. Thus the entire population of channels can be completely described by specifying the numbers of channels $[n_1], [n_2], [n_3], [n_4]$ in the states S_1, S_2, S_3, S_4. Stochastic transitions are considered between the occupation numbers $[n_i]$, $i=1,2,3,4$. Assuming Markov processes for these transitions, a corresponding kinetic scheme can be formalized that explicitly incorporates the stochastic behavior of the ion channels (see Fig. 2).

Similarly, sodium channels can exist in eight different states, and the corresponding kinetic scheme is displayed in Fig. 3, where $[m_i h_j]$ is the number of sodium ion channels with i open activating gates of type m and j open inactivating gates of type h. Thus, $[m_3 h_1]$ denotes the number of open sodium channels. In order to update the state of the population of ion channels with time, we have to create rules in what sequence the states are updated. The simple stochastic methods, described in the preceding section, does not require such rules. In order to enforce positive occupation numbers we update the occupation numbers sequentially, starting with the process with the largest rate and so forth. Let, for example, the transition rate between S_1 and S_2 be $\gamma_{S_1 S_2}$ and the populations of these states be $[n_1]$ and $[n_2]$. Then, the probability p that a channel switches within the time interval $(t, t+\delta t)$ from state S_1 to S_2 is given by $p \equiv \gamma_{S_1 S_2} \delta t$. The probability that $[\delta n_{12}]$ channels switch from state S_1 to state S_2 in the same time interval satisfies the binomial distribution

$$P([\delta n_{12}]) = \binom{[n_1]}{[\delta n_{12}]} p^{[\delta n_{12}]} (1-p)^{([n_1]-[\delta n_{12}])}. \tag{9}$$

Thus the number of switching channels between the states is sequentially drawn from binomial distributions. If the cluster of channels is large, i.e., $[n_1]$ is large, the number of switching channels is also large in the average. Thus, in the time interval δt larger channel clusters experience more transitions.

C. Gillespie's method

Similar as for the Markov process for the occupation numbers, the entire population of ion channels is described at each instant of time by the occupation numbers of all possible states. At any instant of time, the ion channels are distributed over the 13 states, and there are 28 possible transitions (8 transitions for potassium ion channels, 20 transitions for sodium ion channels) to all possible successive states. For each ion channel in state i at time t, the probability of the ion channel remaining in that state in the (sufficiently small) time interval δt is given by $P = e^{-\gamma_i \delta t}$, where γ_i is the sum of all the transition rates from state i to any possible successive state. Sufficiently small means here that during δt no other channel is switching the conductance state. The probability of the cluster of ion channels remaining in the same state in time interval δt is $e^{-\lambda \delta t}$, where

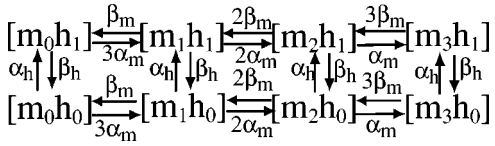

FIG. 3. Kinetic scheme of a stochastic sodium channel.

$$\lambda = \sum_{i=0}^{3} \sum_{j=0}^{1} [m_i h_j] \gamma_{ij} + \sum_{k=0}^{4} [n_k] \gamma_k. \tag{10}$$

Here $[m_i h_j]$ denotes the number of sodium channels in state $m_i h_j$, $[n_k]$ the number of potassium channels in the state n_k, γ_{ij} the total transition rate associated with escaping from state $m_i h_j$, and γ_k the total transition rate associated with escaping from state n_k. For example, for state $m_1 h_1$, $\gamma_{11} = 2\alpha_m + \beta_m + \beta_h$. In order to pick a transition time t_{tr} for a specific ion channel state, one can draw a pseudorandom number r_1 from the uniform distribution [0, 1] and find a transition time by $t_{tr} = \ln(r_1^{-1})/\lambda$. The next step in the stochastic algorithm is to select which of the 28 possible transitions occurs in the time interval t_{tr}. The conditional probability that a particular transition j occurs in the time interval δt is given by

$$\frac{a_j \delta t}{\sum_{i=1}^{28} a_i \delta t} = \frac{a_j}{\sum_{i=1}^{28} a_i}, \tag{11}$$

where a_j is the product of the transition rate associated with transition j and the number of channels in the parent state associated with that transition. Because the sum in the denominator of 11 is a reordered version of 10, it also equals to λ. A specific transition is selected by drawing a random variable r_2 from the uniform distribution $[0, \lambda]$, and determining μ such that

$$\sum_{i=1}^{\mu-1} a_i < r_2 \leqslant \sum_{i=1}^{\mu} a_i. \tag{12}$$

Then we can update the ion channel number in each state, and can update the membrane potential consequently.

D. Langevin approach

Fox and Liu [10,11] have derived the following set of Langevin equations for the gating variables n, m, and h for large ion channel clusters (i.e., when the number of channels in the cluster is large)

$$\frac{d}{dt} n = \alpha_n (1-n) - \beta_n n + \overline{g_n}(t),$$

$$\frac{d}{dt} h = \alpha_h (1-h) - \beta_h h + \overline{g_h}(t),$$

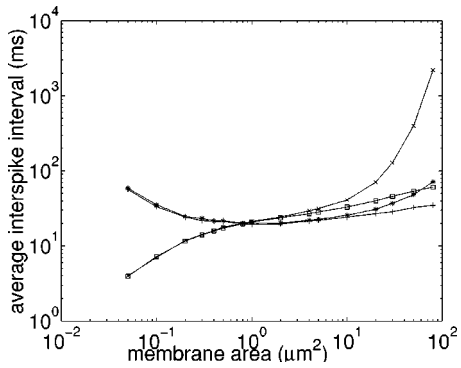

FIG. 4. Comparison of the average time intervals between subsequent action potentials obtained from spike trains of 5000 action potentials for $\sigma=0$ and $\sigma=2\ \ \mu\mathrm{A/cm^2}$. (x): Langevin method at $\sigma=0$, (*): occupation number method at $\sigma=0$, (+): occupation number method at $\sigma=2\ \ \mu\mathrm{A/cm^2}$, (square): Langevin method at $\sigma=2\ \ \mu\mathrm{A/cm^2}$.

$$\frac{d}{dt}m = \alpha_m(1-m) - \beta_m m + \overline{g_m}(t), \tag{13}$$

where the variables $\overline{g_n}(t), \overline{g_h}(t), \overline{g_m}(t)$ denote Gaussian, zero-mean white noise with

$$\langle \overline{g_n}(t)\overline{g_n}(t')\rangle = \frac{2}{N_\mathrm{K}}\frac{\alpha_n(1-n)+\beta_n n}{2}\delta(t-t')$$

$$\langle \overline{g_m}(t)\overline{g_m}(t')\rangle = \frac{2}{N_\mathrm{Na}}\frac{\alpha_m(1-m)+\beta_m m}{2}\delta(t-t')$$

$$\langle \overline{g_h}(t)\overline{g_h}(t')\rangle = \frac{2}{N_\mathrm{Na}}\frac{\alpha_h(1-h)+\beta_h h}{2}\delta(t-t'). \tag{14}$$

Here N_K and N_Na denote the total number of potassium and sodium channels. It is necessary to include restriction to guarantee that m, n, and h do not leave the unit interval [0, 1]. The differential equation for the membrane potential is the classic Hodgkin-Huxley equations where m^3h determines the fraction of open sodium channels and n^4 the fraction of open potassium channels, i.e.,

$$\dot{v} = -\left(\frac{1}{\tau_\mathrm{K}}n^4(v-v_\mathrm{K}^{rev}) + \frac{1}{\tau_\mathrm{Na}}m^3h(v-v_\mathrm{Na}^{rev}) + \frac{1}{\tau_L}(v-v_l)\right) + \xi_s(t). \tag{15}$$

Equations (13)–(15) have to be integrated numerically in order to predict a neuronal spike train. This approach is based on the assumption that the three m gates and the four n gates act each synchronously and can therefore be replaced by single gates each. Furthermore, the resulting master equation is written in terms of a Kramers-Moyal expansion which subsequently is truncated after the diffusion term. The resulting master equation can be converted into an Ito-Langevin equation (see above) or an equivalent Stratonovich-Langevin equation. The error made through these approximations is not controlled and the accuracy has been tested by comparing the results with those obtained by the Markov simulations described above.

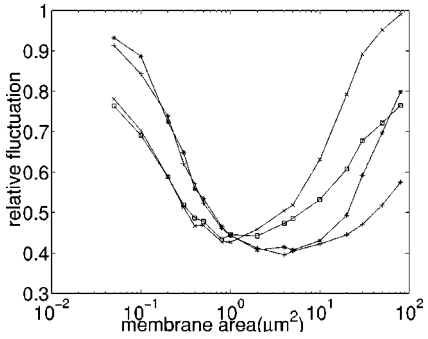

FIG. 5. Comparison of the relative fluctuations [Eq. (21)] of the intervals between subsequent action potentials obtained from spike trains of 5000 action potentials for $\sigma=0$ and $\sigma=2\ \ \mu\mathrm{A/cm^2}$. (x): Langevin method at $\sigma=0$, (*): occupation number method at $\sigma=0$, (+): occupation number method at $\sigma=2\ \ \mu\mathrm{A/cm^2}$, (square):Langevin method at $\sigma=2\ \ \mu\mathrm{A/cm^2}$.

IV. RESULTS

We have compared the average time interval between two subsequent action potentials and the variance obtained from spike trains of 5000 action potentials that have been generated by the methods described above. The simple stochastic scheme, the Markov process method for the occupation number, and the Gillespie method yield results that agree within a 5% error. The Langevin method does not reproduce accurate results (see Figs. 4 and 5). The disagreement is particularly large in the absence of synaptic noise when the average time interval between subsequent spikes diverges for large cluster sizes.

The computation times for the different algorithms are compared in Fig. 6. For the simple stochastic method, the simulation times increase linear with the number of the channels in the cluster. The compute time for the Gillespie method also increases linear in size since the time steps—drawn from an exponential distribution with a linearly decreasing decay time—become smaller as the cluster size increases. The Gillespie method is, however, much more efficient than the simple stochastic method. The occupation number method appears to us as the most efficient method. It

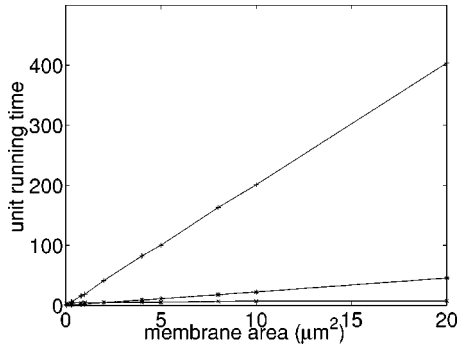

FIG. 6. Comparison of the compute times for clusters of Na^+ and K^+ channels to generate a train of 5000 action potentials using the simple stochastic method (+), the Markov process for the occupation number (x), and the Gillespie method (*).

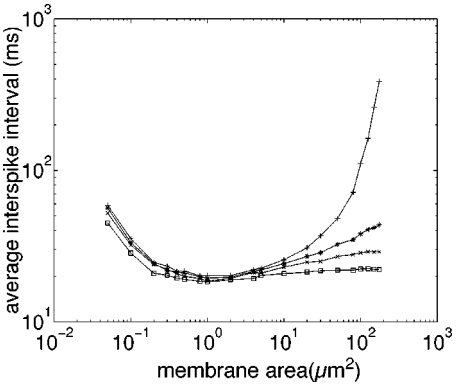

FIG. 7. The average time interval between two subsequent action potentials (in ms) versus membrane area (in μm^2) at $\sigma=0$(+), $\sigma=2$ μA/cm^2 (*), $\sigma=3$ μA/cm^2 (x), and $\sigma=5$ μA/cm^2 (square). These results were obtained with the occupation number method.

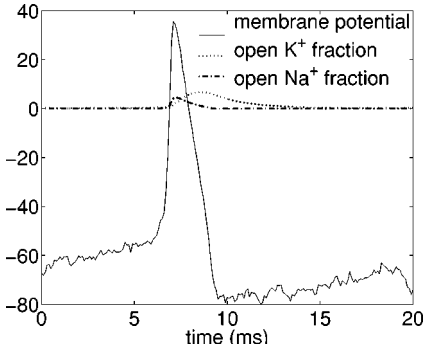

FIG. 8. The membrane potential in millivolt, the fraction of open sodium and potassium channels are shown as a function of time for an ion channel cluster with infinitely many channels. The variance of the external noise is 5 μA/cm^2. For better visibility, the fractions of open channels are multiplied by 20.

leads to faster code with no cost in accuracy since (1) several channels are updated at each time step and (2) the time intervals are fixed independent of the cluster size.

In order to further verify the accuracy of our simulations, we have verified (1) that the results obtained with the stochastic schemes approach the deterministic Hodgkin-Huxley equations when the ion channel number is large and (2) that our results agree with those in Ref. [8].

The Langevin method does not reproduce accurate results for small and large cluster sizes and therefore we did not compare the compute times of this method.

A. Average interspike interval of the ion channel cluster

We consider the combined effect of channel noise and synaptic noise on the average interspike interval $\langle T\rangle$ as shown in Fig. 7 as a function of the cluster size in the absence of an external stimulus. The fraction and density of sodium versus potassium channels are kept constant while the cluster size is increased. In the case of vanishing synaptic noise, the average interspike interval $\langle T\rangle$ first decreases with increasing area of cluster, but then increases again since for infinitely many channels the deterministic Hodgkin-Huxley model is approached. In the presence of synaptic noise, the spiking rate does not decrease to zero as the size of the cluster becomes large. The average spiking rate approaches for large cluster sizes a constant value which is determined by the synaptic noise only. This value, in fact, is *larger* than the spiking rate for small clusters where additional channel noise is present. We thus encounter the paradoxial situation that channel noise in addition to synaptic noise can actually reduce the spontaneous firing rate. To understand this phenomenon it is insightful to consider the two extreme situations of an infinitely large cluster of sodium and potassium channels with synaptic noise and a cluster of three sodium channels and one potassium channel. We set the magnitude of the variance σ of the synaptic noise as 5 μA/cm^2. The membrane potential, the fraction of open sodium ion channels, and the fraction of open potassium ion channels in the case of an infinite cluster size are plotted in Fig. 8. Here the membrane potential fluctuates about its rest state due to the synaptic noise. An action potential is fired when the membrane potential exceeds a threshold (of about −55 mV) which is determined by the deterministic Hodgkin-Huxley equations. The average time interval between two successive spikes is determined by the probability for the membrane potential to cross the threshold.

In the other extreme case, a small cluster of three sodium channels and one potassium channel is considered. The time course of the membrane potential, the number of open sodium channels, and the number of open potassium channels is shown in Fig. 9. As can be seen in Fig. 9(a), an action potential is fired exactly when one sodium channels opens, although the membrane potential is well below the firing threshold of the deterministic Hodgkin-Huxley equations (about −55 mV). In Fig. 9(b), we show a trace of the membrane potential in comparison with the number of open chan-

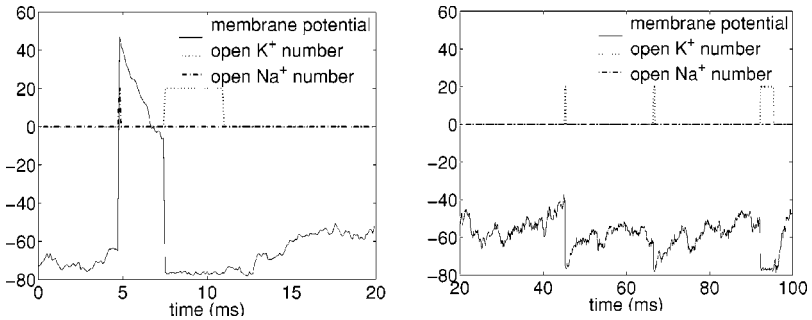

FIG. 9. The membrane potential (in millivolt), the number of open sodium ion channels and the number of open potassium channels are shown as a function of time for the membrane with one potassium channel and three sodium channels. The variance of external noise is 5 μA/cm^2. The number of open channels have been multiplied by a factor of 20.

nels where the membrane potential is well *above* threshold but no action potential is fired. In contrast to the mechanism of action potential generation by large clusters, the mechanism for small clusters is not determined by the firing threshold of the membrane potential, but rather by the single-channel kinetics. To see this we show in the following that the average time for any (of the three) sodium channels of the cluster to open after they all have been reset (after action potential) to a state where all gates are closed agrees well with the average time interval between two successive spikes. In other words, we show that the average interspike interval is determined by the activation time of the sodium channels. A single sodium channel (see Fig. 3) is described by the following set of kinetic equations in which the rates out of the open state m_3h_1 are discarded, i.e., thus generating the cumulative probability $P_o(t)=[m_3h_1]$ for the probability that the channel has opened in the time interval $[0:t]$

$$\frac{d}{dt}[m_0h_1] = \alpha_h[m_0h_0] + \beta_m[m_1h_1] - (\beta_h + 3\alpha_m)[m_0h_1],$$

$$\frac{d}{dt}[m_0h_0] = \beta_h[m_0h_1] + \beta_m[m_1h_0] - (\alpha_h + 3\alpha_m)[m_0h_0],$$

$$\frac{d}{dt}[m_1h_1] = \alpha_h[m_1h_0] + 3\alpha_m[m_0h_1] + 2\beta_m[m_2h_1] - (\beta_m + 2\alpha_m + \beta_h)[m_1h_1],$$

$$\frac{d}{dt}[m_1h_0] = \beta_h[m_1h_1] + 3\alpha_m[m_0h_0] + 2\beta_m[m_2h_0] - (\beta_m + 2\alpha_m + \alpha_h)[m_1h_0],$$

$$\frac{d}{dt}[m_2h_1] = \alpha_h[m_2h_0] + 2\alpha_m[m_1h_1] - (2\beta_m + \alpha_m + \beta_h)[m_ih_1],$$

$$\frac{d}{dt}[m_2h_0] = \beta_h[m_2h_1] + 2\alpha_m[m_1h_0] + 3\beta_m[m_3h_0] - (2\beta_m + \alpha_m + \alpha_h)[m_ih_1],$$

$$\frac{d}{dt}[m_3h_1] = \alpha_h[m_3h_0] + \alpha_m[m_2h_1],$$

$$\frac{d}{dt}[m_3h_0] = \alpha_m[m_2h_0] - (\alpha_h + 3\beta_m)[m_3h_0], \tag{16}$$

with the initial conditions

$$[m_ih_j] = \begin{cases} 1 & \text{for } i=j=0 \\ 0 & \text{otherwise.} \end{cases} \tag{17}$$

Assuming for now that the voltage is clamped, the solution for this set of equations for one single sodium channel is independent of the potassium conductance and can be solved easily for the cumulative probability $P_o(t)$. Since the sodium channels are independent, the cumulative probability that any of the three sodium channels has opened within the time interval $[0:t]$ is given by

$$P_3(t) = 1 - [1 - P_o(t)]^3, \tag{18}$$

and thus the probability density of reopen times of any channel within the cluster of three sodium channels reads

$$\rho_3(t) = \frac{d}{dt}P_3(t) = 3\dot{P}_o(t)[1 - P_o(t)]^2, \tag{19}$$

where the dot indicates a derivative with respect to time t. The average opening time can then be obtained from

$$\langle t_3 \rangle = \int_0^\infty t\rho_3(t)dt. \tag{20}$$

Since the voltage is fluctuating for a cluster of three sodium and one potassium channel (see Figs. 8), the clamped voltage in the rate equations [Eq. (16)] is replaced by the average voltage of −55.49 mV. Plugging the solution of Eq. (16) into Eqs. (17)–(20) one finds the average opening time of 58.18 ms. This number compares favorably with the average interspike interval of 58.71 ms for a cluster of three sodium and one potassium channel obtained by stochastic simulations. This agreement supports the above stated hypothesis that firing of action potentials in small channel clusters is determined by single-channel kinetics and not a threshold of the membrane potential.

As the cluster size is increased, the probability of opening just one sodium ion channel will increase since more sodium channels are available. Thus, the spontaneous firing rate increases with increasing cluster size and the average time interval between subsequent spikes decreases—as can be observed in Fig. 7. When the cluster size further increases, opening of single sodium channels will not always trigger an action potential, a critical fraction of all available sodium channels is required to be open—consistent with the membrane potential crossing a threshold.

Thus the observed reduction of the spontaneous firing rate in spite of additional channel noise reflects a change in the mechanism by which spikes are generated as the ion channel clusters become smaller.

As already mentioned earlier, the Langevin approximation does not accurately reproduce these results.

B. The relative fluctuation of average interspike interval

The variability of the interspike intervals T is described by the relative fluctuations

$$\eta = \frac{\sqrt{\langle (T - \langle T \rangle)^2 \rangle}}{\langle T \rangle}. \tag{21}$$

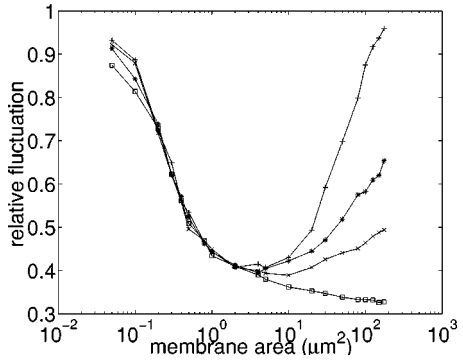

FIG. 10. The relative fluctuations (21) vs membrane area (in μm^2) at $\sigma=0$ (+), $\sigma=2$ $\mu A/cm^2$ (*), $\sigma=3$ $\mu A/cm^2$ (x), and $\sigma=5$ $\mu A/cm^2$ (square). These results were obtained with the occupation number method.

The relative fluctuation of the interspike intervals are plotted versus the cluster size for various values of the strength of the synaptic noise in Fig. 10. In the absence of synaptic noise, the fluctuations of the intervals decrease with increasing cluster size until they reach a minimum. For further increasing cluster sizes, the fluctuations of the intervals increase again (see also Refs. [12,13]). The power spectra of the spike trains shown in Fig. 11 confirm that the spike train exhibits a maximum temporal periodicity at the cluster size where the relative fluctuations are at minimum

The power spectrum of the spike train generated by a membrane with area 0.1 μm^2 is relatively flat. At a membrane area of 5 μm^2 (near the point with minimal relative fluctuation) the power spectrum exhibits a peak close to the angular frequency of 0.37/ms, which corresponds to an average interspike interval of about 17 ms, consistent with the minimum average interspike interval (see Fig. 7). The power spectrum confirms the maximum temporal coherence of the spike train at the same cluster size where the cluster fires action potentials at it's highest rate.

This phenomenon, where optimal coherence is achieved at a certain cluster size resembles somewhat the phenomenon of coherence resonance [17] or autonomous stochastic resonance [18,19] since the intensity of the fluctuations is determined by the size of the cluster. Thus optimizing the size of the cluster is somewhat equivalent to optimizing the noise strength. The relation between these phenomena, however, is not so clear since the relation between cluster size N and noise intensity is not unique as the spontaneous firing rate (a measure of the noise level) exhibits a nonmonotonous behavior.

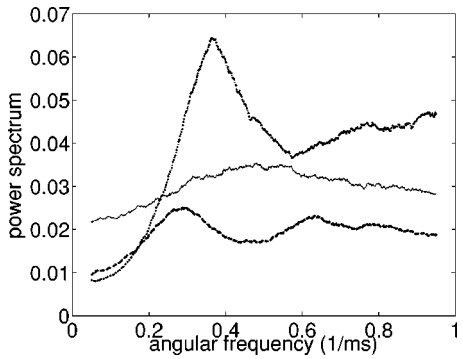

FIG. 11. The power spectrum curves of spike trains generated by membranes with area=0.1 μm^2 (solid line), area=5 μm^2 (dotted line), and area=50 μm^2 (dashed line) in the absence of synaptic noise.

As shown in Fig. 10, synaptic noise alters the relative fluctuations mostly at larger membrane areas, where the channel-noise induced spikes are infrequent. On the other hand, when the area of membrane is small, the statistical features of the neuronal spike train are mainly determined by channel noise.

V. DISCUSSION

We have compared the average interspike interval and the relative fluctuations of trains of action potentials generated by small and large clusters of ion channels. For large ion channel clusters, action potentials are elicited by synaptic noise when the membrane potential exceeds an excitation threshold. For small ion channels clusters, channel noise dominates over synaptic noise. Action potentials are generated at a frequency that is determined by the single-channel kinetics and is only very weakly depending on the synaptic noise strength. We have further shown that at the size of the ion channel cluster at which a maximum spontaneous spiking rate is observed, the spike trains exhibit maximum temporal periodicity. Different stochastic algorithms have been compared. Because the simple stochastic method requires the least number of assumptions it is *a priori* the most accurate method. For spike trains of 5000 spikes the occupation number method and the Gillespie method reproduce the results obtained with the simple stochastic method within 5% error. If the membrane comprises N ion channels, $4N$ random numbers are required for the simple stochastic method. Thus, the simulation time of the simple stochastic method increases linearly with the number of ion channels. In the Gillespie's method, the step time is inversely proportional to λ (15). Since the value of λ is linearly proportional to the number of ion channels number, the simulation step time is inversely proportional to the ion channel number. Thus, the simulation time of the Gillespie's method is also linearly proportional to the number of ion channels—though with a smaller slope than the simple stochastic method. In each simulation step, the occupation-number method needs to generate a fixed number of 28 random numbers regardless of the number of ion channels number. Thus, the simulation time is approximately independent of the number of the ion channels; in our tests it was the fastest method for a given accuracy. The Langevin-method—although designed for large ion channel clusters generates accurate results only for intermediate cluster sizes.

ACKNOWLEDGMENT

This material is based upon work supported by the National Science Foundation under Grant No. IBN-0078055. We thank Jianwei Shuai for fruitful discussions.

[1] A. L. Hodgkin and A. F. Huxley, J. Physiol. (London) **117**, 500 (1952).
[2] E. Neher and B. Sakmann, Nature (London) **260**, 779 (1976).
[3] B. Hille, *Ionic Channels of Excitable Membranes* (Sinauer Associates, Sunderland, MA, 2001).
[4] E. Skaugen and L. Walløe, Acta Physiol. Scand. **107**, 343 (1979).
[5] L. J. DeFelice and A. Isaac, J. Stat. Phys. **70**, 339 (1992).
[6] J. R. Clay and L. J. DeFelice, Biophys. J. **42**, 151 (1983).
[7] C. C. Chow and J. A. White, Biophys. J. **71**, 3013 (1996).
[8] E. Schneidman, B. Freedman, and I. Segev, Neural Comput. **10**, 1679 (1998).
[9] P. N. Steinmetz, A. Manwani, and C. Koch, J. Comput. Neurosci. **9**, 133 (2000).
[10] R. F. Fox and Y. N. Lu, Phys. Rev. E **49**, 3421 (1994).
[11] R. F. Fox, Biophys. J. **72**, 2068 (1997).
[12] P. Jung and J. W. Shuai, Europhys. Lett. **56**(1), 29 (2001).
[13] G. Schmid, I. Goychuk, and P. Hänggi, Europhys. Lett. **56**, 22 (2001).
[14] F. M. Rieke, D. Warland, R. de Ruytervan Steveninck, and W. Bialek, *Spikes: Exploring the Neural Code* (MIT, Cambridge, MA, 1997).
[15] J. A. White, J. T. Rubinstein, and A. R. Kay, Trends Neurosci. **23**, 131 (2000).
[16] A. Manwani and C. Koch, Neural Comput. **11**, 1797 (1999).
[17] A. S. Pikovsky and J. Kurths, Phys. Rev. Lett. **78**, 775 (1997).
[18] H. Gang, T. Ditzinger, C. Z. Ning, and H. Haken, Phys. Rev. Lett. **71**, 807 (1993).
[19] A. Longtin, Phys. Rev. E **55**, 868 (1997).